

The mass function of black holes $1 < z < 4.5$: comparison of models with observations

Priyamvada Natarajan^{1,2} & Marta Volonteri³

¹ *Department of Astronomy, Yale University, New Haven, CT, USA*

² *Institute for Theory and Computation, Harvard-Smithsonian Center for Astrophysics, 60 Garden Street, Cambridge, MA, USA*

³ *Department of Physics and Astronomy, University of Michigan, Ann Arbor, MI, USA*

21 February 2012

ABSTRACT

In this paper, we compare the observationally derived black hole mass function (BHMF) of luminous ($> 10^{45} - 10^{46}$ erg/s) broad-line quasars (BLQSOs) at $1 < z < 4.5$ drawn from the Sloan Digital Sky Survey (SDSS) presented in Kelly et al. (2010), with models of merger driven BH growth in the context of standard hierarchical structure formation models. In the models, we explore two distinct black hole seeding prescriptions at the highest redshifts: "light seeds" - remnants of Population III stars and "massive seeds" that form from the direct collapse of pre-galactic disks. The subsequent merger triggered mass build-up of the black hole population is tracked over cosmic time under the assumption of a fixed accretion rate as well as rates drawn from the distribution derived by Merloni & Heinz (2008). Four model snapshots at $z = 1.25$, $z = 2$, $z = 3.25$, $z = 4.25$ are compared to the SDSS derived BHMFs of BLQSOs. We find that the light seed models fall short of reproducing the observationally derived mass function of BLQSOs at $M_{\text{BH}} > 10^9 M_{\odot}$ throughout the redshift range; the massive seed models with a fixed accretion rate of $0.3 E_{\text{dd}}$, or with accretion rates drawn from the Merloni & Heinz distribution provide the best fit to the current observational data at $z > 2$, although they overestimate the high-mass end of the mass function at lower redshifts. At low redshifts, a drastic drop in the accretion rate is observed and this is explained as arising due to the diminished gas supply available due to consumption by star formation or changes in the geometry of the inner feeding regions. Therefore, the over-estimate at the high mass end of the black hole mass function for the massive seed models be easily be modified, as the accretion rate is likely significantly lower at these epochs than what we assume. For the Merloni & Heinz (2008) model, examining the Eddington ratio distributions f_{Edd} , we find that they are almost uniformly sampled from $f_{\text{Edd}} = 10^{-2} - 1$ at $z \simeq 1$, while at high redshift, current observations suggest accretion rates close to Eddington, if not mildly super-Eddington, at least for these extremely luminous quasars. Our key findings are that the duty cycle of SMBHs powering BLQSOs increases with increasing redshift for all models and models with Pop III remnants as black hole seeds are unable to fit the observationally derived BHMFs for BLQSOs, lending strong support for the massive seeding model.

1 INTRODUCTION

Demography of local galaxies suggests the that most galaxies harbour a quiescent super-massive black hole (SMBH) in their nucleus at the present time and the mass of the hosted SMBH is correlated with properties of the host bulge. Observational evidence supports the existence of a strong connection between the growth of the central SMBH and stellar assembly of the host spheroid (Tremaine et al. 2002; Ferrarese & Merritt 2000; Gebhardt et al. 2000; Marconi & Hunt 2003; Haring & Rix 2004; Gültekin et al. 2009) and possibly the host halo in nearby galaxies (Ferrarese 2002). This strong correlation is suggestive of co-eval growth of the BH and the stellar component likely via regulation of the gas

supply in galactic nuclei from the earliest times (Silk & Rees 1998; Kauffmann & Haehnelt 2000; Fabian 2002; King 2003; Thompson, Quataert & Murray 2005; Natarajan & Treister 2009; Treister et al. 2011). Meanwhile, our observational understanding of accreting black holes and their properties at high redshifts $z > 6$ is growing (see Fan et al. 2010 for an overview). Black holes appear to be copiously accreting and in place before the universe was a billion years old as evidenced by the recent detection of the quasar at $z = 7.085$ in the UKIDSS survey reported by Mortlock et al. (2011). Our access to the earliest redshifts is of course restricted to the brightest candidates, optical, and deep X-ray surveys

are needed to uncover the potentially highly obscured population at these epochs (Treister et al. 2011).

Simultaneously our theoretical understanding of the assembly history of black holes over cosmic time has been rapidly improving (see recent reviews by Volonteri 2010 and Natarajan 2011). With the increasing availability of observations from earlier and earlier epochs, models can be effectively tested at extremely high redshifts. Recently, a more complete census of the accreting black hole population at $1 < z < 4.5$ has become available enabling the estimate of the mass function (MF) of these black holes (Kelly et al. 2010, K10 hereafter). In this paper, we explore a range of theoretically viable models to fit this additional and new data-set.

Observations currently provide strong constraints locally, and hints at high redshifts (Mortlock et al. 2011; Treister et al. 2011). With this additional anchor during intermediate epochs ($z \sim 1-4$), discrimination between models finally starts becoming possible as we demonstrate here. In particular, we are able to distinguish between seed black hole formation scenarios. This paper is the third in a series (Volonteri, Lodato & Natarajan 2008, and Volonteri & Natarajan 2009, VLN08 and VN09 respectively hereafter) where we compare the late time evolution of SMBH seeds, focusing on the difference between a population of more numerous, but smaller mass BHs as seeds, versus a population of rarer, but more massive initial seeds. The outline of this paper is as follows: in Section 1, we briefly review the new observations and BHMFs derived therefrom; Section 2 provides the context of the theoretical black hole growth models followed by a description of how BHMFs are derived in Section 3; and finally we present the results of comparing observations to the models and the derived conclusions.

2 BHMFS FROM OBSERVATIONS AND MODELS

K10 derive an estimate of the BHMF of BLQSOs correcting for incompleteness and statistical uncertainties from a sample of 9886 quasars at $1 < z < 4.5$ from the SDSS. They find ‘downsizing’ of BHs in BLQSOs, i.e. the peak of the number density shifts to higher redshift with increasing black hole mass peaking at $z \sim 2$. They report that as a function of black hole mass and Eddington ratio, the SDSS at $z > 1$ is highly incomplete at $M_{\text{BH}} \leq 10^9 M_{\odot}$ and $L/L_{\text{Edd}} < 0.5$. The lower limit on the lifetime of a single BLQSO phase was estimated to be $> 150 \pm 15$ Myr, with a maximum black hole mass of $\sim 3 \times 10^{10} M_{\odot}$. K10 also find that the Eddington ratio distribution peaks at $L/L_{\text{Edd}} \sim 0.05$ with a dispersion of ~ 0.4 dex implying that most BLQSOs are radiating nowhere near or at the Eddington limit. From their estimated lifetime and Eddington ratio distributions they also infer that most massive black holes spend a significant amount of time growing in an earlier obscured phase consistent with models of self-regulated growth. The recent claimed discovery of a population of heavily obscured, copiously accreting black holes at $z \geq 6$ by Treister et al. (2011) provides an interesting glimpse perhaps of the precedents of the SDSS BLQSOs population at lower redshifts. Note that this claim of a detection of a copiously accreting and obscured population of black holes at $z > 6$ on X-ray

image stacking by Treister et al. (2011) as well as its significance have been disputed by Cowie et al. (2011) and Willott (2011). The issue can only be settled conclusively with more high redshift data that will hopefully be forthcoming. As noted in our earlier work, in particular, VN09, with more comprehensive observational redshift coverage, several key assumptions in the modeling approaches can be tested.

In this paper we focus our modeling efforts on four redshifts of interest ($z = 1.25$; $z = 2$; $z = 3.25$; $z = 4.25$; to match the redshift bins in K10). At each redshift our models provide us with a sample of all SMBHs present at that particular cosmic time, and of the SMBHs that are actively accreting. From the SMBH mass and its Eddington ratio, f_{Edd} , we can derive their bolometric luminosity: $\log(L_{\text{bol}}/\text{erg s}^{-1}) = 38.11 + \log(M_{\text{BH}}/M_{\odot}) + \log(f_{\text{Edd}})$. We apply a bolometric correction of 4.3 (as in K10) and select only quasars that are more luminous than the minimum luminosity determined by the flux limit described in Richards et al. (2006), the parent sample of K10. The threshold bolometric luminosities corresponding to each bin are as follows. At $z = 1.25$, $\log(L_{\text{bol}}/\text{erg s}^{-1})=44.7$; at $z = 2$: $\log(L_{\text{bol}}/\text{erg s}^{-1})=45.2$; at $z = 3.25$: $\log(L_{\text{bol}}/\text{erg s}^{-1}) = 45.5$; at $z = 4.25$: $\log(L_{\text{bol}}/\text{erg s}^{-1})=45.8$. Finally, we assume that the fraction of unobscured quasars is 20%, based on La Franca et al. (2005). Here we do not explicitly apply the evolutionary model of La Franca et al. (2005), where the fraction of obscured quasars depends on both redshift and luminosity, as the redshift range we are interested is beyond that explored by La Franca et al. (2005), but we note that when we apply their evolutionary model to the redshift range $z = 1-3$, adopting the bolometric corrections of Marconi et al. (2004), we obtain consistent results. Recently Fiore et al. (2012) have also derived and published BHMFs for the entire active SMBH population as opposed to just the BLQSOs as done by K10.

3 BLACK HOLE GROWTH MODELS

To trace the assembly history of black holes with cosmic time, Monte-Carlo realizations are performed to derive the merger histories of dark matter haloes. We also trace the formation and growth of embedded black holes as a function of cosmic time as outlined below.

3.1 Black hole seeds

To track the mass assembly history of black holes in the universe, we need to start with seeds at high redshift. In the standard picture, the assumption is that the remnants of the massive first stars (Pop III stars) provide the earliest seeds in the range of $50-100 M_{\odot}$. We note here that whether the first stars were indeed this massive has been called to question from the latest round of recent higher resolution simulation results where fragmentation occurs ubiquitously (Turk et al. 2009; Greif et al. 2011; Davis et al. 2011). An alternate model for the formation of massive seeds from the direct collapse of pre-galactic disks is presented in Lodato & Natarajan (2007; 2006). In these models, there is a limited mass range of halos with a further narrow range in spins that are able to form seeds. However, contrary to the Pop III case, massive seeds with $M \approx 10^5 - 10^6 M_{\odot}$ can form at high redshift ($z > 15$),

when the intergalactic medium has not been significantly enriched by metals (Koushiappas et al. 2004; Begelman et al. 2006; Lodato & Natarajan 2006, 2007). More details of this seeding model can be found in Lodato & Natarajan (2006, 2007), wherein the development of non-axisymmetric spiral structures drives mass infall and accumulation in a pregalactic disc with primordial composition. The central mass accumulation that provides an upper limit to the SMBH seed mass that can form is given by:

$$M_{\text{BH}} = m_{\text{d}} M_{\text{halo}} \left[1 - \sqrt{\frac{8\lambda}{m_{\text{d}} Q_{\text{c}}} \left(\frac{j_{\text{d}}}{m_{\text{d}}} \right) \left(\frac{T_{\text{gas}}}{T_{\text{vir}}} \right)^{1/2}} \right] \quad (1)$$

for

$$\lambda < \lambda_{\text{max}} = m_{\text{d}} Q_{\text{c}} / 8 (m_{\text{d}} / j_{\text{d}}) (T_{\text{vir}} / T_{\text{gas}})^{1/2} \quad (2)$$

and $M_{\text{BH}} = 0$ otherwise. Here λ_{max} is the maximum halo spin parameter for which the disc is gravitationally unstable, m_{d} is the gas fraction that participates in the infall and Q_{c} is the Toomre parameter. The efficiency of SMBH formation is strongly dependent on the Toomre parameter Q_{c} , which sets the frequency of formation, and consequently the number density of SMBH seeds. Guided by our earlier investigation, we set $Q_{\text{c}} = 2$ (the intermediate efficiency massive seed model) as described in VLN08.

The efficiency of the seed assembly process ceases at large halo masses, where the disc undergoes fragmentation instead. This occurs when the virial temperature exceeds a critical value T_{max} , given by:

$$\frac{T_{\text{max}}}{T_{\text{gas}}} = \left(\frac{4\alpha_{\text{c}}}{m_{\text{d}}} \frac{1}{1 + M_{\text{BH}}/m_{\text{d}} M_{\text{halo}}} \right)^{2/3}, \quad (3)$$

where $\alpha_{\text{c}} \approx 0.06$ is a dimensionless parameter measuring the critical gravitational torque above which the disc fragments (Rice, Lodato & Armitage 2005).

To summarize the seeding model, every dark matter halo is characterized by its mass M (or virial temperature T_{vir}) and by its spin parameter λ . The gas has a temperature $T_{\text{gas}} = 5000\text{K}$. If $\lambda < \lambda_{\text{max}}$ (see eqn. 2) and $T_{\text{vir}} < T_{\text{max}}$ (eqn. 3), then we assume that a seed BH of mass M_{BH} given by eqn. (1) forms in the center. The remaining relevant parameters are $m_{\text{d}} = j_{\text{d}} = 0.05$, $\alpha_{\text{c}} = 0.06$ and here we consider the $Q_{\text{c}} = 2$ case. In the massive seed model, SMBHs form (i) only in haloes within a narrow range of virial temperatures ($10^4 \text{ K} < T_{\text{vir}} < 1.4 \times 10^4 \text{ K}$), hence, halo velocity dispersion ($\sigma \simeq 15 \text{ km s}^{-1}$), and (ii) for a given virial temperature all seed masses below $m_{\text{d}} M$ modulo the spin parameter of the halo are allowed (see eqns. 1 and 3). The seed MF peaks at $10^5 M_{\odot}$, with a steep drop at $3 \times 10^6 M_{\odot}$. We refer the reader to Lodato & Natarajan (2007) and VLN08 for a discussion of the mass function (and related plots). Here we stress that given points (i) and (ii) above, the initial seeds do not satisfy the local $M_{\text{BH}} - \sigma$ relation, in fact the seed masses are not correlated with σ , rather they are correlated with the spin parameter of the dark matter halo.

In this paper, we once again contrast this model with a popular scenario that advocates the first black holes are the remnants of zero metallicity stars. We assume that one Pop III star forms in metal-free halos with $T_{\text{vir}} > 2000 \text{ K}$ (Yoshida et al. 2006). We assume a logarithmically flat initial MF, $dN/d \log M = \text{const}$, between $10 M_{\odot}$ and $600 M_{\odot}$, where the upper limit comes from Omukai & Palla (2003),

and suppose that seed black holes form when the progenitor star is in the mass range $40 - 140 M_{\odot}$ or $260 - 600 M_{\odot}$ (Fryer et al. 2001). The remnant mass is taken to be one-half the mass of the star.

Both scenarios for black hole seed formation rely on zero metallicity gas. We model the evolution of metallicity by the ‘high feedback, best guess’ model of Scannapieco et al. (2003). Scannapieco et al. (2003) model metal enrichment via pair-instability supernovae winds, by following the expansion of spherical outflows into the Hubble flow. They compute the co-moving radius, at a given redshift, of an outflow from a population of supernovae that exploded at an earlier time. Using a modification of the Press–Schechter technique, Scannapieco & Barkana (2002) compute the bivariate MF of two halos of arbitrary mass and collapse redshift, initially separated by a given co-moving distance. From this function they calculate the number density of supernovae host halos at a given co-moving distance from a ‘recipient’ halo of a given mass M_h that form at a given redshift z . By integrating over this function, one can calculate the probability that a halo of mass M_h forms from metal-free gas at a redshift z . When a halo forms in our merger tree we calculate the probability that it is metal-free (hence, it can form Pop III stars) and determine if this condition is satisfied.

Every halo entering the merger tree is assigned a spin parameter drawn from the lognormal distribution in λ_{spin} found in numerical simulations, with mean $\bar{\lambda}_{\text{spin}} = 0.05$ and standard deviation $\sigma_{\lambda} = 0.5$ (Davis & Natarajan 2009). We assume that the spin parameter of a halo is not modified by its merger history, as no consensus exists on this issue at the present time.

3.2 Black hole growth

We evolve the population of SMBH seeds according to simple models of self-regulation with the host. The main features of the models have been discussed elsewhere (Volonteri & Natarajan 2009). We summarize below all the relevant modeling assumptions. SMBHs in galaxies undergoing a major merger (i.e., having a mass ratio $> 1 : 10$) accrete mass and become active. Each SMBH accretes an amount of mass, $\Delta M = 9 \times 10^7 (\sigma / 200 \text{ km s}^{-1})^{4.24} M_{\odot}$, where σ is the velocity dispersion after the merger. This relationship scales with the $M_{\text{BH}} - \sigma$ relation, as it is seen today (Gültekin et al. 2009):

$$M_{\text{BH}} = 1.3 \times 10^8 \left(\frac{\sigma}{200 \text{ km s}^{-1}} \right)^{4.24} M_{\odot}; \quad (4)$$

the normalization in ΔM was chosen to take into account the contribution of SMBH-SMBH mergers, without exceeding the mass given by the $M_{\text{BH}} - \sigma$ relation.

We link the correlation between the black hole mass and the central stellar velocity dispersion of the host with the empirical correlation between the central stellar velocity dispersion and the asymptotic circular velocity as $\sigma = v_{\text{c}} / \sqrt{2}$ of galaxies (?). The latter is a measure of the total mass of the dark matter halo of the host galaxy. We calculate the circular velocity from the mass of the host halo and its redshift.

The rate at which mass is accreted scales with the Edington rate for the SMBH, and we set either a fixed Ed-

dington ratio of $f_{\text{Edd}} = 1$ (for Pop III seeds), $f_{\text{Edd}} = 0.3$ (for massive seeds), or an accretion rate derived from the distribution derived by Merloni & Heinz (2008) (we apply this model to massive seeds only). The empirical distribution of Eddington ratios derived by Merloni & Heinz (2008, MH08 thereafter) is fit by a function in $\log(L_{\text{bol}}/L_{\text{Edd}})$. The fitting function of the Eddington ratio distribution as a function of SMBH mass and redshift, is computed in 10 redshift intervals (from $z = 0$ to $z = 5$) for 4 different mass bins ($6 < \log(M_{\text{BH}}/M_{\odot}) < 7$; $7 < \log(M_{\text{BH}}/M_{\odot}) < 8$; $8 < \log(M_{\text{BH}}/M_{\odot}) < 9$; $9 < \log(M_{\text{BH}}/M_{\odot}) < 10$), and then fit with an analytic function which is the sum of a Schechter function and a log-normal (A. Merloni, private communication). The Eddington ratio distributions are then normalized to unity at every given mass and redshift. We dub the three models **PopIII-Edd**, **Massive-MH** and **Massive-subEdd** respectively. Note that in the model names the first part refers to the type of seed and the second part refers to the kind of accretion history assumed. Therefore the model **PopIII-Edd** refers to: initial seeds from Pop III remnants always accreting at the Eddington rate; model **Massive-MH** refers to initial massive seeds accreting with Eddington ratios drawn from the MH08 distribution and the model **Massive-subEdd**: initial massive seeds accreting 0.3X Eddington at all times.

In the **Massive-MH** model the accretion rate is not limited to the Eddington rate and mildly super-Eddington accretion rates (up to $f_{\text{Edd}} \sim 10$) are possible and allowed as per MH08.

For all three scenarios considered here, accretion starts after a dynamical timescale at the virial radius, $t_{\text{dyn}} = 10^8 \text{ yr } (R_{\text{vir}}/100 \text{ kpc})(v_{\text{vir}}/100 \text{ km s}^{-1})^{-1}$, and lasts until the SMBH, of initial mass M_{in} , has accreted ΔM . The lifetime of an AGN therefore depends on how much mass it accretes during each episode:

$$t_{\text{AGN}} = \frac{t_{\text{Edd}}}{f_{\text{Edd}}} \frac{\epsilon}{1 - \epsilon} \ln\left(\frac{M_{\text{fin}}}{M_{\text{in}}}\right), \quad (5)$$

where ϵ is the radiative efficiency ($\epsilon \simeq 0.1$), $t_{\text{Edd}} = 0.45 \text{ Gyr}$ and $M_{\text{fin}} = \min[(M_{\text{in}} + \Delta M), 1.3 \times 10^8 (\sigma/200 \text{ km s}^{-1})^{4.24} M_{\odot}]$.

We further assume that, when two galaxies hosting SMBHs merge, the SMBHs themselves merge within the merger timescale of the host halos, which is a plausible assumption for SMBH binaries formed after gas-rich galaxy mergers Dotti et al. (2007). We adopt the relations suggested by Taffoni et al. (2003) for the merger timescale. Black holes are allowed to accrete during the merging process if the timescale for accretion, corresponding to the sum of the dynamical timescale and t_{AGN} , is longer than the merger timescale.

As outlined earlier, in propagating the seeds it is assumed that accretion episodes and therefore growth spurts are triggered only by major mergers. We find that in a merger-driven scenario for SMBH growth the most biased galaxies at every epoch host the most massive SMBHs that are most likely already sitting on the $M_{\text{BH}} - \sigma$ relation. Lower mass SMBHs (below $10^6 M_{\odot}$) are instead off the relation at $z = 4$ and even at $z = 2$. These baseline results are **independent of the seeding mechanism**. In the initial massive seeds scenario, most of the SMBH seeds start out **well above** the $z = 0$ $M_{\text{BH}} - \sigma$ relation, that is, they are

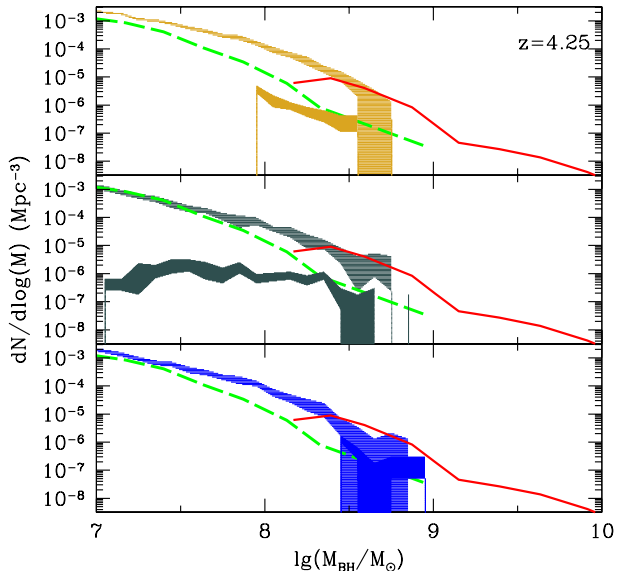


Figure 1. The derived MF of SMBHs at $z = 4.25$. The upper shaded curve in all three panels is the MF for all SMBHs including active and inactive ones. The lower (darker) shaded curve in all three panels is the MF for SMBHs that can be identified as BLQSOs. The dashed curve in all three panels is the MF of all SMBHs from MH08. The solid curve is the MF of BLQSOs from K10. The three panels refer to the models: **PopIII – Edd** (uppermost panel), **Massive – MH** (middle panel), **Massive – subEdd** (bottom panel).

‘over massive’ compared to the local relation. Seeds form only in haloes within a narrow range of velocity dispersion ($\sigma \simeq 15 \text{ km s}^{-1}$ at the earliest epochs, see eqns. 1 and 3). The SMBH mass corresponding to $\sigma \simeq 15 \text{ km s}^{-1}$, according to the local $M_{\text{BH}} - \sigma$ relation, would be $\sim 3 \times 10^3 M_{\odot}$. The MF instead peaks at $10^5 M_{\odot}$ (Lodato & Natarajan 2007). As time elapses, all haloes are bound to grow in mass by mergers. The lowest mass haloes, though, experience mostly minor mergers, that do not trigger accretion episodes, and hence do not grow the SMBH. The evolution of these systems can be described by a shift towards the right of the $M_{\text{BH}} - \sigma$ relation: σ increases, but M_{BH} stays roughly constant.

4 RESULTS AND CONCLUSIONS

In what follows, we present a detailed comparison of the data with our three models, namely the **PopIII-Edd**: initial seeds from Pop III remnants with accretion assumed at all times at the Eddington rate; **Massive-MH**: wherein the initial massive seeds have accretion rates drawn from the distribution determined by MH08; **Massive-subEdd**: initial massive seeds with accretion assumed at all times to be at 0.3× the Eddington rate. For all three models, we compare our derived MF of BLQSOs with that estimated by K10 and the MF of all SMBHs (the entire population that includes actively accreting + inactive black holes) with the MF predicted by MH08. Although the latter is also a theoretical MF, it is derived under completely different assumptions,

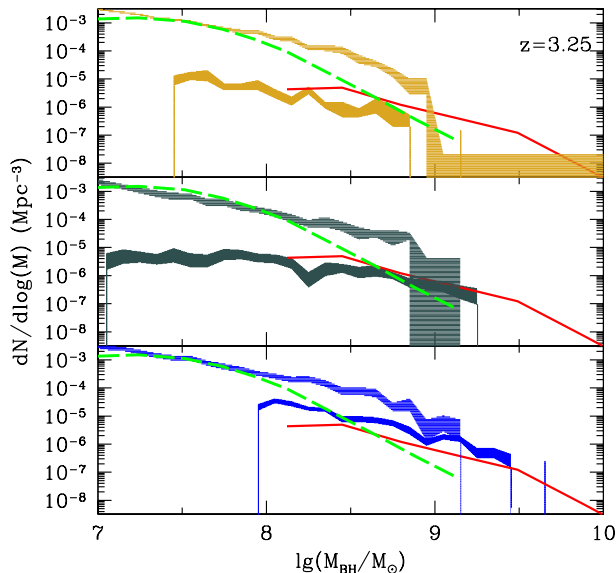


Figure 2. The derived MF of SMBHs at $z = 3.25$. The upper shaded curve in all three panels is the MF for all SMBHs including active and inactive ones. The lower (darker) shaded curve in all three panels is the MF for SMBHs that can be identified as BLQSOs. The dashed curve in all three panels is the MF of all SMBHs from MH08. The solid curve is the MF of BLQSOs from K10. The three panels refer to the models: **PopIII – Edd** (uppermost panel), **Massive – MH** (middle panel), **Massive – subEdd** (bottom panel).

as the MH08 model starts with SMBHs today and evolves them back in time via a continuity equation. We therefore consider this an interesting case of model confronting model (see also Volonteri & Begelman 2010).

We compare our derived MFs for BLQSOs to K10 and our MFs for the entire BH population (active + inactive) to MH08 in Figures 1-4. We find the following:

- In the higher redshift slices at $z = 4.25$ and $z = 3.25$, independent of our models the MF derived in MH08 for all SMBHs is incompatible with that for the subset of BLQSOs from K10. In these instances the abundance of BLQSOs from K10 is in excess of that of all SMBHs from MH08 models. It is only in the lowest redshift bin at $z = 1.25$ that the MFs of BLQSOs from K10 is lower than that of all SMBHs derived from the MH08 models. It is therefore clear that the Eddington ratio distributions derived from K10 and from MH08 are most likely discrepant.

- At the highest redshift slice $z = 4.25$, the light seed model **PopIII-Edd** shown in the top panel fails to grow SMBHs massive enough (more massive than $\sim 10^{8.5} M_\odot$) to populate the high-mass end of the MF of BLQSOs of K10. The discrepancy is roughly two orders of magnitude as clearly seen in the upper panel of Figure 1. Since the Eddington ratio was assumed to be unity to evolve this model, a deficit at the high mass end cannot be compensated for by altering the accretion physics any further. Alternatively, if SMBHs can become “over massive” at higher z (i.e., if they climb well above the standard $M_{\text{BH}} - \sigma$ relation) and have phases of super-Eddington accretion (Volonteri & Rees

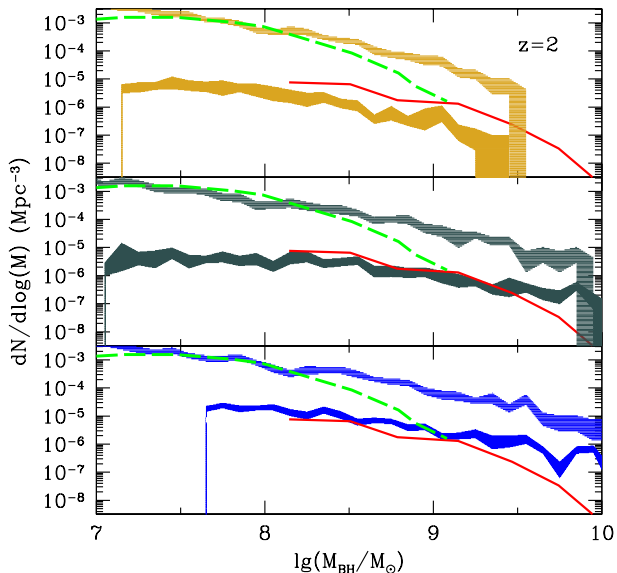


Figure 3. The derived MF of SMBHs at $z = 2$. The upper shaded curve in all three panels is the MF for all SMBHs including active and inactive ones. The lower (darker) shaded curve in all three panels is the MF for SMBHs that can be identified as BLQSOs. The dashed curve in all three panels is the MF of all SMBHs from MH08. The solid curve is the MF of BLQSOs from K10. The three panels refer to the models: **PopIII – Edd** (uppermost panel), **Massive – MH** (middle panel), **Massive – subEdd** (bottom panel).

2005), then enough SMBHs at the high mass end might be produced. We note that assuming the MH08 accretion model in conjunction with Pop III remnants (this model is not plotted in our figures) makes the discrepancy at the high mass end much worse, as the accretion rate for low mass black holes ($< 1000 M_\odot$) in the MH08 model peaks at sub-Eddington rates at all redshifts.

- Both the massive seed models (**Massive-subEdd** and **Massive-MH**) also under-produce the K10 MFs at the highest redshift slice as seen clearly by looking at the middle and bottom panels in $z = 4.25$;

- The MF of all existing SMBHs (active + inactive) from the **PopIII-Edd**, **Massive-subEdd** and **Massive-MH** models overestimates MH08’s MF for all SMBHs at all masses $> 3 \times 10^7 M_\odot$ at $z = 3.25$, while there is reasonably good agreement with K10 for the BLQSO MF for the **Massive-MH** model.

- At lower redshifts ($z = 1.25$ and $z = 2$) both massive seed models start to overestimate the MF of BLQSOs by K10 at $M_{\text{BH}} > 10^9 M_\odot$. This is not unexpected, as we have not implemented a cut-off to mimic the depletion of available gas in massive galaxies.

- All massive seeds models (**Massive-subEdd** and **Massive-MH**) overestimate the MF of all SMBHs (active + inactive) from MH08 at $M_{\text{BH}} > 10^{8.5} M_\odot$. At $z < 2$ we cannot clearly assess whether MH08 might underestimate the total MF. We are, however, inclined to attribute the discrepancy to our models, for the same reason that we likely overestimate the MF of quasars as we do not take into account

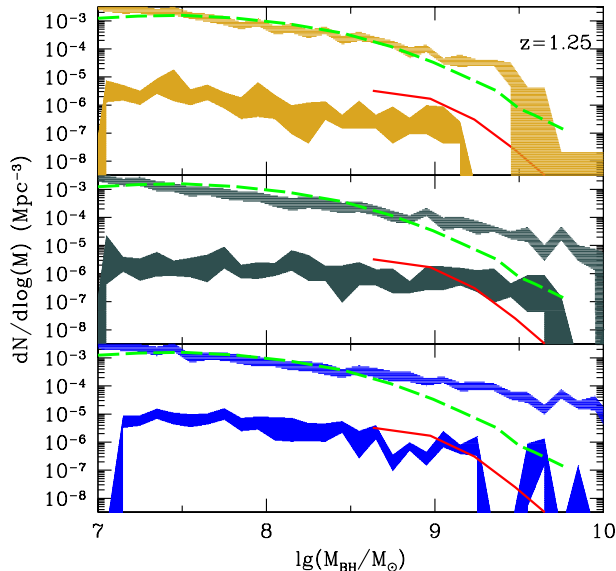


Figure 4. The derived MF of SMBHs at $z = 1.25$. The upper shaded curve in all three panels is the MF for all SMBHs including active and inactive ones. The lower (darker) shaded curve in all three panels is the MF for SMBHs that can be identified as BLQSOs. The dashed curve in all three panels is the MF of all SMBHs from MH08. The solid curve is the MF of BLQSOs from K10. The three panels refer to the models: **PopIII – Edd** (uppermost panel), **Massive – MH** (middle panel), **Massive – subEdd** (bottom panel).

changes in the gas inventory at late times in the universe. The **PopIII-Edd** model gets instead into better alignment at lower and lower redshifts. At $z = 2$ these MFs begin to agree up to $10^8 M_\odot$ and at $z = 1.25$ they fall into excellent agreement up to $10^9 M_\odot$.

- For model **Massive-MH** we can estimate the typical Eddington ratio of SMBHs powering BLQSOs. We find that most luminous quasars at the highest redshift have accretion rates close to or even slightly larger than the Eddington rate (the fraction of super-Eddington accreting SMBHs is $\simeq 60\%$ at $z = 3$; $\simeq 40\%$ at $z = 2$; $\simeq 20\%$ at $z = 1$). At lower redshift, the flux limit of the SDSS survey corresponds to lower luminosities, and less powerful accretors are selected. In general, we find that the accretion rates in the models overestimate the accretion rates derived by K10.

- We estimate the duty cycle, defined as the fraction of SMBHs that are active and detectable as BLQSOs, and show the results for the three models (**PopIII-Edd**, **Massive-subEdd**, **Massive-MH**) in Figure 5 at $z = 1$, $z = 2$, $z = 3$, $z = 4$ (dark to light shade of colours). Comparing the theoretical duty cycle with the duty cycle estimated by K10 at $z = 1$, we find that model **PopIII-Edd** is consistent at all masses; while models **Massive-MH** and **Massive-Edd** overestimate the duty cycle at $M_{\text{BH}} > 10^9 M_\odot$ (as expected from the MF shown in Figures 3 and 4).

- We find that the duty cycle increases with increasing redshift for all our models, although more strongly for the **Massive-subEdd** model. This is due to the fact that this model is the one with the lowest average accretion rate

($f_{\text{Edd}} = 0.3$, versus $f_{\text{Edd}} = 1$ for the **PopIII-Edd** and $f_{\text{Edd}} \gtrsim 1$ in **Massive-MH** at $z > 3$, therefore, from Equation 5 the BHs in the **Massive-subEdd** model need to accrete for a longer time in order to reach the final mass set by the $M_{\text{BH}} - \sigma$ relation.

In conclusion, the implications for seeding models are that light seeds always under-produce the bright end of the BLQSO LF for high black hole masses. This is a serious issue as they are assumed to be already accreting at the optimal Eddington rate.

Moreover, according to recent work (Turk et al. 2009; Greif et al. 2011; Davis et al. 2011) it appears now that (i) the IMF of the first stars may not be biased high as fragmentation might occur during the formation process and (ii) due to turbulence the formation of the first stars might get delayed. So the **PopIII-Edd** model aside from being unable to match the black hole MF derived from BLQSOs from the SDSS as shown here, might in fact not be the most efficient channel to produce seeds. It is clear that a channel to form more massive black hole seeds at high redshifts is required to start matching observations of the bright end (massive end of the black hole MF) from the earliest to intermediate redshifts ($z \sim 1$), and not only at the highest redshifts as previously noted (e.g., Haiman 2004; Yoo & Miralda-Escudé 2004; Shapiro 2005; Volonteri & Rees 2005, 2006). **Therefore, low-mass SMBH seeds such as Pop III star remnants require exceptional growth conditions not only to explain the existence of rare objects such as $z > 6$ quasars, but also to explain the unexceptional population of luminous quasars at $z \simeq 2 - 3$.**

Over-predicting the BHMF at the high mass end is typically not a serious problem as lowering the Eddington rate would fix that. For instance, Natarajan & Treister (2009) propose the existence of an upper mass limit to BHs at all epochs, arising from the shutting off of accretion due to self-regulation of the gas supply in the galactic nuclei. According to their estimate this upper limit is given by:

$$M_{\text{BH}} \sim 5 \times 10^9 \left(\frac{\sigma}{350 \text{ km s}^{-1}} \right)^5 M_\odot. \quad (6)$$

K10 estimate an upper mass limit at $z \sim 1$ for a black hole hosting a BLQSO to be $M_{\text{BH}} \sim 3 \times 10^{10} M_\odot$. Utilizing the limit proposed by Natarajan & Treister (2009), if a BH shuts off at the end of this BLQSO episode at $z \sim 1$, it is likely hosted in a galaxy with a velocity dispersion of $\sigma \sim 440$ km/s, which corresponds to the typical velocity dispersion of the brightest central galaxy in a cluster. This fits in nicely with the view of down-sizing wherein accretion is noted to shut off at $z \sim 1$ in these BCGs in clusters.

ACKNOWLEDGEMENTS

PN acknowledges support from the John Simon Guggenheim Foundation and a residency at the Rockefeller Bellagio Center where a portion of this work was completed. She also thanks the Institute for Theory and Computation at Harvard for hosting her during her Guggenheim Fellowship year.

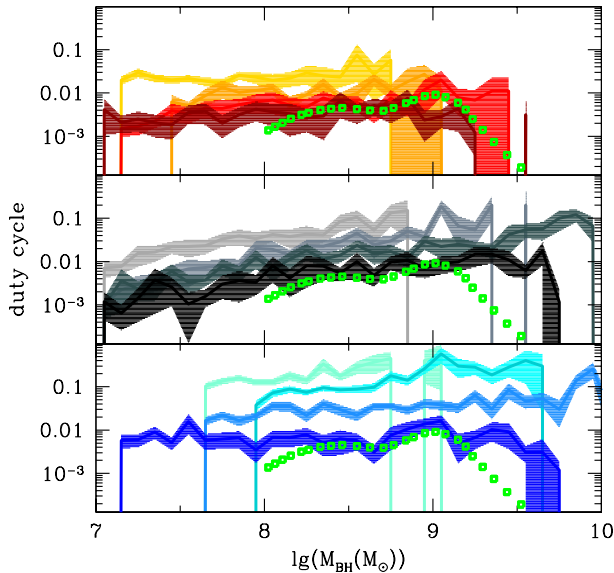


Figure 5. The duty cycle of BLQSOs as a function of SMBH mass. The models shown here are again in the same order as before: **PopIII – Edd** (uppermost panel), **Massive – MH** (middle panel), **Massive – subEdd** (bottom panel). In each panel, we show the duty cycle at $z = 4$, $z = 3$, $z = 2$, and $z = 1$ (from lightest to darkest shade respectively). The square symbols show the lower bound on the duty cycle at $z = 1$ from K10.

REFERENCES

- Baes M., Buyle P., Hau G. K. T., Dejonghe H., 2003, MNRAS, 341, L44
 Begelman M. C., Volonteri M., Rees M. J., 2006, MNRAS, 370, 289
 Cowie L. L., Barger A. J., Hasinger G., 2012, ApJ, in press (arXiv1110:3326)
 Davis, A; Smith, B; & Natarajan, P., 2011, in preparation
 Dotti M., Colpi M., Haardt F., Mayer L., 2007, MNRAS, 379, 956
 Ferrarese L., 2002, ApJ, 578, 90
 Ferrarese L., & Merritt, D., 2000, ApJ, 578, 90
 Fiore S., et al., 2012, A&A, 537, 16
 Fryer C. L., Woosley S. E., Heger A., 2001, ApJ, 550, 372
 Greif, T., White, S., Klessen, R., & Springel, V., 2011, preprint, arXiv1101.5493
 Gültekin K., Richstone D. O., Gebhardt K., Lauer T. R., Tremaine S., Aller M. C., Bender R., Dressler A., Faber S. M., Filippenko A. V., Green R., Ho L. C., Kormendy J., Magorrian J., Pinkney J., Siopis C., 2009, ApJ, 698, 198
 Haiman, Z. 2004, ApJ, 613, 36
 Kelly B. C., Vestergaard M., Fan X., Hopkins P., Hernquist L., Siemiginowska A., 2010, ApJ, 719, 1315
 Koushiappas S. M., Bullock J. S., Dekel A., 2004, MNRAS, 354, 292
 Lodato G., Natarajan P., 2006, MNRAS, 371, 1813
 Lodato G., Natarajan P., 2007, MNRAS, 377, L64
 Marconi A., Hunt L., 2003, ApJ, 598, L21
 Marconi A., Risaliti G., Gilli R., Hunt L. K., Maiolino R., Salvati M., 2004, MNRAS, 351, 169

- Merloni A., Heinz S., 2008, MNRAS, 388, 1011
 Mortlock D., et al., 2011, Nature, 474, 616
 Omukai K., Palla F., 2003, ApJ, 589, 677
 Pizzella A., Corsini E. M., Dalla Bontà E., Sarzi M., Coccato L., Bertola F., 2005, ApJ, 631, 785
 Rice K., Lodato G., & Armitage P., 2005, MNRAS, 364, L56
 Richards G., et al., 2006, AJ, 131, 2766
 Scannapieco E., Barkana R., 2002, ApJ, 571, 585
 Scannapieco E., Schneider R., Ferrara A., 2003, ApJ, 589, 35
 Shapiro, S. L. 2005, ApJ, 620, 59
 Taffoni G., Mayer L., Colpi M., Governato F., 2003, MNRAS, 341, 434
 Tremaine S., et al., 2002, ApJ, 574, 740
 Turk, M., Abel, T., & O’Shea, B., 2009, Science, 325, 601
 Volonteri, M., & Rees, M. J. 2005, ApJ, 633, 624
 Volonteri, M., & Rees, M. J. 2006, ApJ, 650, 669
 Volonteri M., Natarajan P., 2009, MNRAS, 400, 1911
 Willott, C. J. 2005, ApJ, 742, L8
 Yoo, J., & Miralda-Escudé, J. 2004, ApJ, 614, L25
 Yoshida N., Omukai K., Hernquist L., Abel T., 2006, ApJ, 652, 6